The International Journal of Cardiovascular Imaging (2019) 35:947–954
https://doi.org/10.1007/s10554-019-01527-7

ORIGINAL PAPER

Assessment of artery calcification in atherosclerosis with dynamic 18F-FDG-PET/CT imaging in elderly subjects

Mamdouh S. Al-enezi[1,3] · Redha-alla Abdo[1] · Mohamed Yazid Mokeddem[1] · Faiçal A. A. Slimani[1] · Abdelouahed Khalil[2] · Tamas Fulop[2] · Eric Turcotte[1] · M'hamed Bentourkia[1]

Received: 12 October 2018 / Accepted: 3 January 2019 / Published online: 2 February 2019

Abstract
Glucose metabolism in atherosclerotic arteries has been shown to be an indicator of inflammation, which might be a precursor of plaque rupture. In this prospective study, we assessed the correlation between artery calcification and glucose metabolism by means of 18F-FDG PET/CT imaging in elderly subjects. Nineteen elderly subjects, with age ranging from 65 to 85 years, underwent CT and dynamic 18F-FDG-PET imaging. The artery calcification was determined with a threshold of 130 Hounsfield units. Intensity of calcification and ratio of calcification area to total artery area were classified in four sequential classes from CT images. The CT artery images were also classified as having single or multi-spot calcifications. Their respective glucose metabolism was assessed with fractional uptake rate (FUR). Factor analysis was used in this study to separate blood images from tissue to extract the blood time activity curves for FUR calculations. The artery images in PET data were corrected for partial volume effect. The total arterial segments analyzed were 1332, with 1085 without calcification (81%), 247 (19%) with calcification, and 94 segments were having multi-spot of calcifications. There was a statistically significant difference in FUR values between non-calcified to calcified segments and between subjects under medication to non-medication when comparing the subjects based on calcification area. No statistically significant differences of FUR were found between single spot as a function of intensity, while in the multi-spots, there was a statistically significant difference for all artery segments. Metabolism activity varies for non-calcified to calcified segments. Based on the metabolic activity represented by FUR, calcifications in multi-spots have different effects than in single spots.

Keywords Atherosclerosis · Calcification · Arteries · Plaque · PET · PET/CT · 18F-FDG

Introduction

Atherosclerosis is a vascular inflammatory disorder and is considered a major cause of cardiovascular diseases and severe events including sudden death [1]. It is characterized by the accumulation of inflammatory cells and oxidized lipids within the vessel wall, causing the construction of the plaque [2–4].

✉ M'hamed Bentourkia
mhamed.bentourkia@usherbrooke.ca

1 Department of Nuclear Medicine and Radiobiology, Faculty of Medicine and Health Sciences, University of Sherbrooke, 3001, 12th Avenue North, Sherbrooke, QC J1H 5N4, Canada

2 Department of Medicine, Faculty of Medicine and Health Sciences, University of Sherbrooke, Sherbrooke, QC, Canada

3 Department of Diagnostic Radiology, Faculty of Applied Medical Science, University of Hail, Hail, Saudi Arabia

The plaque development is a long and dynamic slow process, which might complicate the effort for early diagnosis. Therefore, there is neither standardized approach for early diagnosis nor for plaque stability level [5]. Identifying the vulnerable plaque would reduce atherosclerosis-associated disability and mortality, however this is yet remaining a major ongoing challenge.

Pharmacological lipid lowering therapy by means of statins and other preventives are available, however, residual risk remains even in patients treated with preventive drug therapies [6–8].

Lumenographic techniques, like intravascular ultrasound, digital subtraction angiography and magnetic resonance angiography allow for absolute quantification of the plaque and its components, but they are still unable to detect vulnerable plaque [5, 8, 9].

In the hematological point of view, there are several systemic inflammatory biomarkers being established for

atherosclerosis inflammation, among them the C-reactive protein (CRP) which is correlated with increased risk of cardiac events [10, 11]. Unfortunately, the biomarkers together with CRP suffer poorness of information in terms of the plaque localization, level of stabilization and specificity to atherosclerotic inflammation.

Framingham is one example of diagnostic criteria available for identifying population at risk, with low reliability for an individual patient and lack of differentiability of acute cardiovascular risk and chronic stable risk [11, 12].

Most of the analytical studies in regard of atherosclerosis disease are for oncology patients, while the impact of anticancer medical therapies in tracer uptake could influence the accuracy and reproducibility of the analysis [13]. Moreover, neglecting the effect of partial volume might cause noticeable influence on the accuracy of quantitative PET analysis, especially for artery size less than two times the scanner spatial resolution at full width at half maximum [14].

In the present work, we report the correlation between 18F-FDG uptake in the arteries as a function of plaque intensity and calcification area with single and multi-spots of calcifications. These parameters were also evaluated as a function of medication with Rosuvastatin and medication for chest angina.

Materials and methods

Subjects' measurements

We recruited 10 subjects with age ranging from 65 to 85 years (69.15 ± 3.7). These subjects were imaged twice at 12 months apart for a total of 19 PET/CT scans (one subject was measured only once). In the rest of this paper, the returning subjects were considered as new subjects resulting in a total of 19 subjects as we do not report the changes in atherosclerosis during the 12-month period. The subjects were classified as with non-medication and under-medication groups. 4 subjects were under medication for 1 year and they were taking Rosuvastatin 20 mg/day. 5 subjects were having chest angina and they were taking their own prescribed anti-inflammatory drugs. In total, at the PET/CT scans, 10 subjects were non-medicated and 9 were under-medication. All the subjects were non-smokers and not having excessive alcohol consumption, not taking antioxidants, vitamin supplements or hormonal replacement for women.

The measurement of glucose, total cholesterol, low density lipoprotein, high density lipoprotein, triglyceride and CRP were performed in each subject after overnight fasting. Subjects were injected intravenously with an 18F-FDG bolus at an activity of 140 to 400 MBq depending on the subject's weight. PET and CT were performed with a PET/CT system (Philips Gemini TF 16). Imaging started with non-enhanced low-dose CT (120 kV) which was used for PET attenuation correction and artery calcification detection. CT images were reconstructed in sets of transaxial 512×512 matrices with a pixel size of 1 mm × 1 mm × 5 mm. The PET scans were initiated in dynamic mode for 30 min and were divided into 26 consecutive time frames of 12×10 s; 8×30 s; 6×240 s. In dynamic mode means the subjects were injected with a bolus of 18F-FDG simultaneously with the initiation of PET scanning. PET slices were reconstructed into a 144×144 matrix, and the voxel size was 4 mm × 4 mm × 4 mm. The arteries scanned were the aorta and left and right iliacs. In total, 118 image slices were acquired with CT and 45 slices, i.e. one bed position, with PET in dynamic mode. The aorta and iliacs were identified on each CT and PET image slice and their correspondence on CT and PET was established based on their location in mm as read from CT and PET image file header.

Image analysis

CT images were evaluated visually for the presence of vascular calcification defined according to a threshold of 130 Hounsfield units (HU) for the disclosure of calcification [15]. Thereafter, each lesion was classified within intensity intervals in HU based on the Agatston scale [15].

The classes of intensities (CI) in the CT artery image were defined as: CI0, with no calcification, i.e. pixel intensities below 130 HU; CI1, intensities between 130 and 199 HU; CI2, 200–299 HU; CI3, 300–399 HU; and CI4, intensity > 400 HU.

The area of calcification was measured for each artery segment as a ratio of calcification area (RCA), defined as an area of at least 2 adjacent pixels > 130 HU to total arterial area and expressed as a percentage (%) [16, 17]. Subsequently, the RCAs were subdivided in four classes as for CI with the help of the Ward's clustering method [18]: RCA0 = absence of calcification; RCA1: ⩽ 10%; RCA2: 11–20%; RCA3: 21–30%; RCA4: > 30%.

Fractional uptake rate (FUR) was used in this study to quantify 18F-FDG uptake in PET images. It is an approximated value to Patlak slope and is independent of the body size and gender [19]. FUR was evaluated as $\mathrm{FUR} = \frac{\mathrm{C(T)}}{\int_0^{\mathrm{T}} \mathrm{Cp(t)dt}}$ with T the time at the mid-frame time, $C(T)$ and $C_p(t)$ are the PET artery image count and input function, respectively [20]. The FUR calculations were done on PET images of the last 3 data points of the time activity curve, i.e. from frame times corresponding to the last 12 min of the scan (from 18 to 30 min).

Since most published works reported the values of tissue-to-blood ratio (TBR) for static PET imaging, we calculated TBR and included its values as an indication together with FUR values. TBR was assessed as the ratio of the standard

uptake value (SUV) of tissue ROI to SUV of artery blood pool ROI [21, 22] extracted from factor analysis of blood image component [23].

Notwithstanding that the circulation time is short, FUR is recognized as an approximation to the Patlak slope (Ki) estimated from dynamic measurements [24, 25], the later showed an excellent agreement between 30 min and the standard 60-min imaging protocol, while SUV may vary widely with the time of measurement after the intravenous injection of 18F-FDG (and therefore TBR) [26]. Reference [24] reported a 98% correlation between FUR and Patlak Ki while only 61% between SUV and Ki, and suggested a time of 15–20 min post-injection sufficient to calculate FUR in tumors with PET dynamic acquisitions. From the aforementioned studies, we assumed the time would not affect the FUR calculations.

Factor analysis (FA) was used to derive the input function from the sagittal view of the aorta (Fig. 1) [27].

For partial volume correction purposes, artery diameter were extracted from CT transaxial images of pixel size 1 mm × 1 mm. For PET images, the artery diameter was assessed from the first 60 s of the dynamic transaxial PET images where the images were mainly made of blood, and also from the FA blood images. In this case, the images of the arteries were fitted with 2D Gaussians and the full-width at half maximum (FWHM) averaged in the two orthogonal directions were assumed as artery diameter [28]. The artery transaxial images in PET measurements were corrected for partial volume effect based on the study in [29] made in our center using 18F-FDG and the same PET/CT scanner.

The measurement of the mean in the region of interest (ROI) was made over the pixels in the ROI having intensity above 70% of ROI maximum to avoid the influence of image noise for single pixel measurement as well as background contribution [30].

We have corresponded the CT and PET slices by matching their slice positions to avoid interpolation uncertainties during image co-registration. The analyses were then performed on the 512 × 512 CT images and on the 144 × 144 PET images.

Statistical analysis

The statistical analyses were performed with the aid of analysis of variance ANOVA for unpaired multi-groups and with the Student t-test for the comparison of unpaired two groups. A p value < 5% was considered statistically significant.

Results

The subject characteristics are reported in Table 1 as a function of non-medication and under-medication. CRP was the indicator of inflammation commonly used in the clinic. Its high value confirmed the presence of inflammation in subjects under-medication. FUR and TBR in last rows are discussed in the next paragraphs.

The total arterial segments analyzed in this study were 1332, with 1085 segments were not calcified (81%) and 247 (19%) were having calcification. 153 (62%) of the calcified segments were occupied with a single-spot (SS) calcification (Table 2), and 94 (38%) with multi-spot calcifications (MS) (Table 3). The 94 artery segments with MS had a total of 231 calcification

Table 1 Subjects' characteristics averaged for non-medication and under-medication

	Non-medication	Under-medication
Age (years)	69.58 ± 3.93	69.92 ± 2.32
Weight (kg)	71.0 ± 5.62	84.1 ± 18.62
Total cholesterol (mmol/L)	5.90 ± 0.48	3.75 ± 0.56
HDL (mmol/L)	1.35 ± 0.21	1.24 ± 0.21
LDL (mmol/L)	3.87 ± 0.51	1.96 ± 0.44
Triglycerides (mmol/L)	1.45 ± 0.48	1.22 ± 0.21
Glucose (mmol/L)	4.58 ± 0.36	5.06 ± 0.29
CRP (mg/L)	3.03 ± 0.045	6.27 ± 3.28
FUR*	0.0842 ± 0.0348	0.0672 ± 0.0209
TBR*	2.4343 ± 0.8736	2.1516 ± 0.7773

The values are expressed as mean ± standard deviation, and the symbol * means p-value < 5%

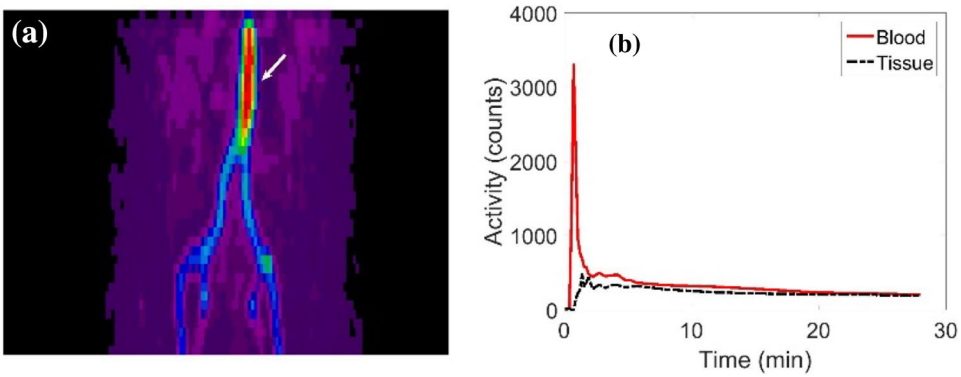

Fig. 1 **a** Sagittal view of the blood FA image with aorta indicated with the white arrow. **b** Blood and tissue time activity curves extracted from aorta FA images

Table 2 Distribution of ratio of artery calcification (RCA) versus classes of intensities (CI) for single-spot (SS) artery calcification

	RCA1	RCA2	RCA3	RCA4	Total
CI1 or SS1	30	3	2	0	35
CI2 or SS2	22	27	1	0	50
CI3 or SS3	1	13	9	8	31
CI4 or SS4	0	6	18	13	37
Total segments	53	49	30	21	153

Table 3 Distribution of ratio of artery calcification (RCA) versus classes of intensities (CI) for multi-spot (MS) artery calcifications

	RCA1	RCA2	RCA3	RCA4	Total
CI1 or MS1	75	2	1	0	78
CI2 or MS2	52	13	2	0	67
CI3 or MS3	12	17	12	3	44
CI4 or MS4	10	17	10	5	42
Total segments	149	49	25	8	231

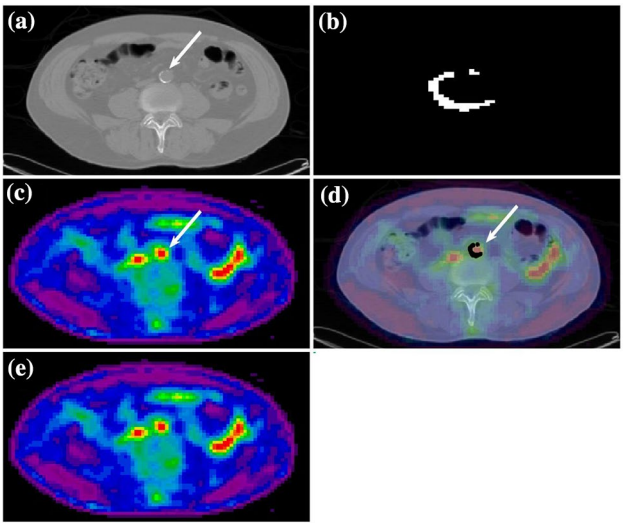

Fig. 2 **a** CT image with calcified aorta (white arrow). **b** Segmented calcification spots. **c** Corresponding PET image slice with the aorta indicated with the white arrow. **d** Fused PET/CT for display only, with overlapping FDG signal and calcification (black arc) (white arrow). **e** FUR image resembling to image in **c** but with low intensity. All displayed images were differently zoomed

spots. From Table 2 for SS, it appears that most calcifications with smaller area have low intensity, and those with larger area have high intensity. In the case of MS artery calcifications, the calcifications were found made mostly of smaller areas. The largest area (RCA4) was found in only 8 segments with MS calcifications, independently of their intensity.

Figure 1 depicts an example of the decomposition with FA into blood and tissue of a PET artery image. The blood curve in Fig. 1b was used as the input function in FUR calculation. Figure 2 shows an example of CT image of the aorta having two spots of calcification and its corresponding PET image. The CT and PET images were matched based on their scanning slice positions. Figure 3 shows an artery with 4 calcification spots segmented with active contours and classified from 1 to 4 based on their mean intensities.

The statistical comparison between non-calcified and calcified arteries showed a statistically significant difference in their FUR values (FUR mean of non-calcified = 0.0827 and 0.0727 of calcified, $p < 0.05$; TBR mean of non-calcified = 2.434 and 2.152 of calcified, $p < 0.05$) (Fig. 4a). In this figure, the calcified data included the single-spot and multi-spot calcifications and the artery segments of subjects under medication and non-medication. Figure 4b was obtained in the same manner as in Fig. 4a but without inclusion of arteries of subjects under medication, and still the two sets of data were found statistically significantly different (FUR mean of non-calcified = 0.0829 and 0.0762 of calcified, $p < 5\%$; TBR mean of non-calcified = 2.434 and 2.024 of calcified, $p < 5\%$). Figure 4c was obtained in all calcified artery segments but classified as having calcifications with single spots (SS) versus those having multi-spots (MS) (FUR mean for calcified SS = 0.0752 and for calcified MS = 0.0838, $p = 0.017$). However, for TBR, the difference between SS and MS was not significant ($p > 5\%$). We also compared SS FUR versus MS FUR in artery segments from non-medicated subjects and in subjects under medication and found that the statistical difference between SS FUR and MS FUR in artery segments from non-medicated subjects was not significant ($p = 0.39$; mean SS FUR = 0.0808; mean MS FUR = 0.0854), while the difference was statistically significant between SS FUR and MS FUR in artery segments from subjects under medication ($p = 0.018$; mean SS FUR = 0.0708; mean MS FUR = 0.0824). Finally, by comparing all artery segments of subjects not under medication to those a long time under medication, excluding the subjects who took Rosuvastatin for 12 months, the difference was found statistically significant (FUR mean non-medication = 0.0842 and for under medication 0.0672, $p < 5\%$). From these data, it can be concluded that: (1) medication lowers uptake of 18F-FDG in the arteries; (2) in the absence of medication, the calcification lowers 18F-FDG uptake; and (3) artery segments with multi-spot calcifications accumulates more 18F-FDG than those with single spot calcification.

Figure 5a shows FUR values for the four intensity classes (CI) of arteries having single-spot calcification in the medicated and non-medicated subjects. Figure 5b depicts the FUR values as a function of the four classes of area ratios (RCA) still in the arteries with a single spot calcification. From these figures, and apart from the values in Fig. 5a for CI3, the results show a decline of glucose metabolism in

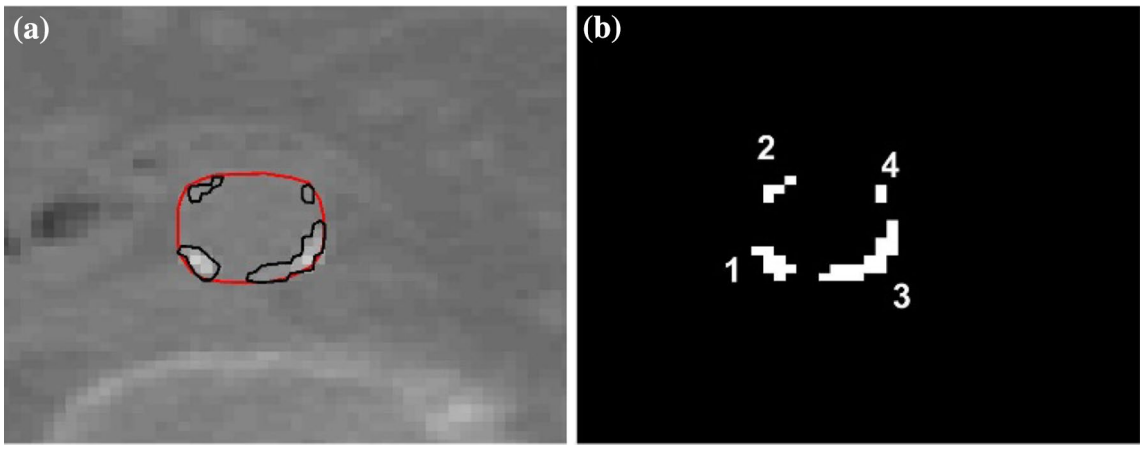

Fig. 3 **a** CT artery image with multi-spot calcifications extracted by utilizing active contour. **b** The numbers on each spot represent its class corresponding to their mean CT HU numbers

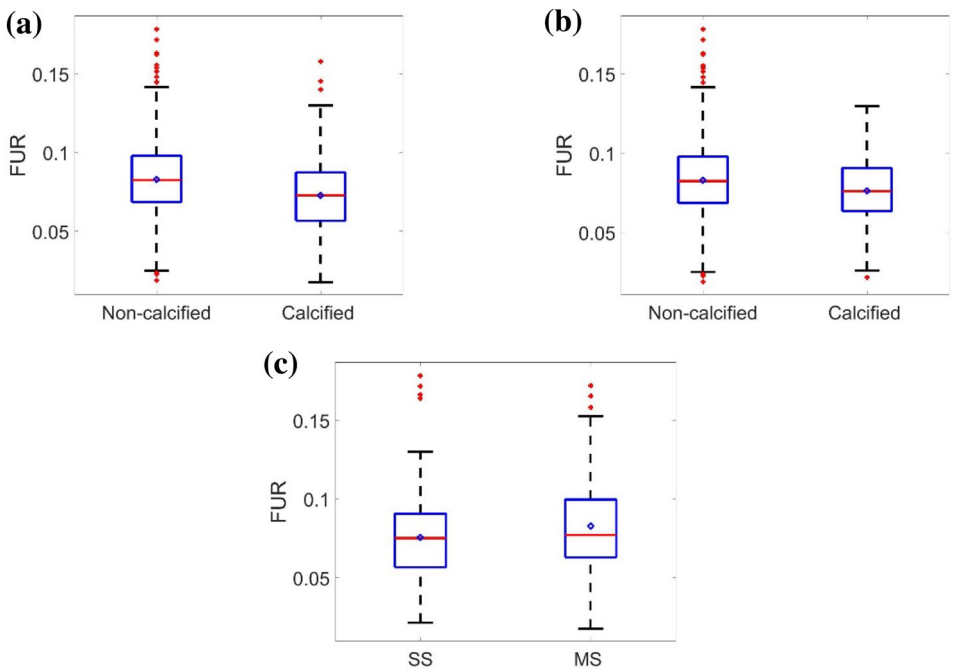

Fig. 4 **a** FUR for non-calcified to calcified segments ($p < 0.05$; mean non-calcified = 0.0827; mean calcified = 0.0727). All artery segments were included. The circle near the line of the median indicates the mean. The dots above and below the quantiles represent outliers. **b** Same as in **a** but with excluding artery segments of subjects under medication ($p < 0.05$; mean non-calcified = 0.0829; mean calcified = 0.0762). **c** Comparison of all calcified artery segments as having single calcification spot SS versus those having multi-spot calcifications MS ($p < 0.05$; mean SS = 0.0752; mean MS = 0.0838)

high intensity calcification and in large area calcification for single-spot calcifications. The statistical difference between non-medication to under-medication was not significantly different based on intensity ($p = 0.24$, Fig. 5a), while it was different based on the area ratios ($p = 0.0089$, Fig. 5b).

By grouping artery segments for SS and MS calcifications, and by plotting FUR as a function of intensity classes CI and area classes RCA, the medication were still shown to lower FUR (Fig. 6). FUR values appeared with a slight increase as a function of the extent of the calcification.

The difference between the two groups under medication, i.e. subjects using Rosuvastatin (20 mg/day) (N = 4 with 189 artery segments) and subjects using their prescribed anti-inflammatory drugs (N = 5 with 386 artery segments), and considering the total arterial segments, were found significantly different for FUR and for TBR (FUR mean = 0.077 ± 0.041 versus 0.083 ± 0.035, $p = 0.032$; TBR mean 3.67 ± 1.64 versus 4.46 ± 1.22, $p < 0.05$, for Rosuvastatin and anti-inflammatory groups respectively).

Discussion

The present study aims were to show how 18F-FDG varies with calcification intensity and volume in subjects under medication and non-medication. We identified each

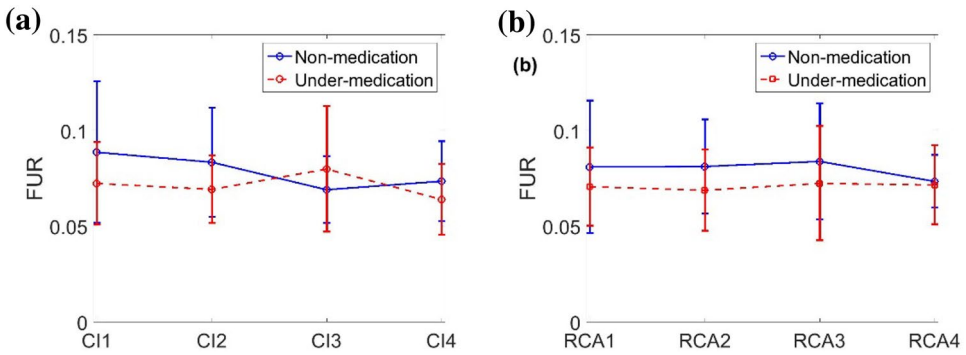

Fig. 5 **a** FUR values in the four intensity classes of arteries identified with single-spot (SS) calcification. **b** Same in the four area classes. In both figures, the curves were shown in groups of subjects with and without medication. The differences of the means between non-medication and under-medication were not statistically significantly different for calcification intensity in **a** ($p=0.24$), but they were different in **b** ($p=0.0089$)

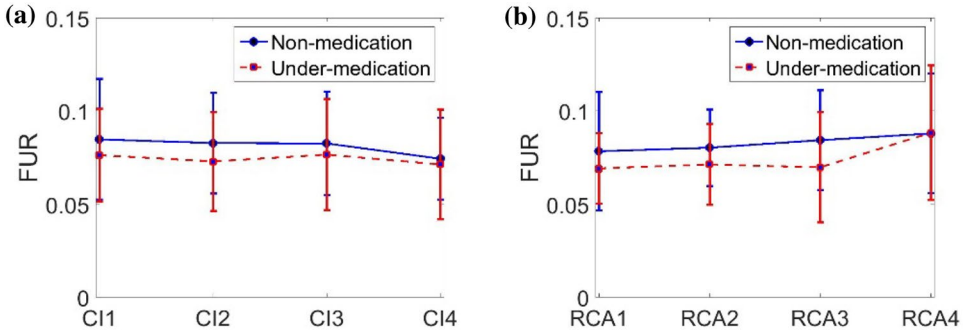

Fig. 6 **a** FUR values for mixed SS and MS versus the four intensity classes (CI). **b** Same in the four area classes. In overall, medication lowers FUR, and high intensity calcifications show decreased FUR while large area calcifications tend to increase FUR

calcification with its intensity and volume without the recourse to image coregistration. There was a confirmation of the clear statistical difference provided by the effect of medication as demonstrated in the literature [8, 31].

The difference between artery segments having single spot or multi-spot calcifications, and between those having small or large volume, have to be considered at the same level as calcification scores [12, 15]. We demonstrated in this work that calcifications with high intensity and/or with large volume in a single spot calcification behave differently from arteries with multi-spot calcifications. The rise of 18F-FDG uptake in multi-spot calcification arteries, i.e. with larger volume, might be due to its exposure to high level of shear stress which can result in plaque instability [6]. In the same point of view, it has been reported that microcalcifications within the plaque would produce an increase in peak circumferential stress, transforming the plaque into a vulnerable plaque [32, 33]. Finally, the calcification was suggested to be associated with remodeling and plaque expansion, but without inflammation [34], translating a low uptake of 18F-FDG.

The present data showed that uptake of 18F-FDG is lower in calcified than in non-calcified arteries as was also reported in the literature [13, 35, 36]. However, artery segments with multi-spot calcifications were found to have higher 18F-FDG uptake than in artery segments with single-spot calcification, suggesting more metabolically active plaques reflecting plaques rich in macrophages [9].

Despite the modest number of subjects involved in this prospective study with dynamic PET imaging (10 without medication and 9 under medication for artery inflammation), the artery calcifications classified as single spot (153 artery segments) and multi-spots (94 artery segments), in addition to 1085 artery segments without calcification, were separately analysed for their 18F-FDG uptake. One of the findings in this work suggests that in order to detect an active artery plaque (vulnerable plaque), it is recommended to consider the plaques individually in the same artery segment concurrently using CT and PET images. The other findings were related to 18F-FDG uptake versus artery calcifications/non-calcification and calcification intensity and volume independently in each artery segment.

Conclusion

Metabolism activity varies for non-calcified to calcified segments and with medication. FUR for multi-spot calcification correlated with larger calcification area. Under the point of

view of metabolic activity represented by FUR, calcifications with multi-spots may have different effect than single spot.

Acknowledgements We are grateful to the Canadian Institutes of Health Research (CIHR) for their financial support, and to the Saudi Arabian culture bureau in Canada and University of Hail in kingdom of Saudi Arabia for the fellowship to Mr. Al-enezi.

Compliance with ethical standards

Conflict of interest There are no conflict of interest.

References

1. Virmani R, Kolodgie FD, Burke AP, Finn AV, Gold HK, Tulenko TN. Wrenn SP (2005) Atherosclerotic plaque progression and vulnerability to rupture angiogenesis as a source of intraplaque hemorrhage. Arter Thromb Vasc Biol 25(10):2054–2061
2. Libby P, Ridker PM, Hansson GK (2009) Inflammation in atherosclerosis: from pathophysiology to practice. J Am Coll Cardiol 54(23):2129–2138
3. Osborn EA, Kessinger CW, Tawakol A, Jaffer FA (2017) Metabolic and molecular imaging of atherosclerosis and venous thromboembolism. J Nucl Med 58:871–877. https://doi.org/10.2967/jnumed.116.182873
4. Costopoulos C, Liew TV, Bennett M (2008) Ageing and atherosclerosis: mechanisms and therapeutic options. Biochem Pharmacol. https://doi.org/10.1016/j.bcp.2007.10.006
5. Naghavi M, Madjid M, Khan MR et al (2001) New developments in the detection of vulnerable plaque. Curr Atheroscler Rep 3(2):125–135
6. Nighoghossian N, Derex L, Douek P (2005) The vulnerable carotid artery plaque: current imaging methods and new perspectives. Stroke 36:2764–2772. https://doi.org/10.1161/01.STR.0000190895.51934.43
7. Pugliese G, Iacobini C, Fantauzzi CB, Menini S (2015) The dark and bright side of atherosclerotic calcification. Atherosclerosis 238:220–230. https://doi.org/10.1016/j.atherosclerosis.2014.12.011
8. Revkin JH, Shear CL, Pouleur HG et al (2007) Biomarkers in the prevention and treatment of atherosclerosis: need, validation, and future. Pharmacol Rev 59:40–53. https://doi.org/10.1124/pr.59.1.1
9. Owen DR, Lindsay AC, Choudhury RP, Fayad ZA (2011) Imaging of atherosclerosis. Annu Rev Med 62:25–40. https://doi.org/10.1146/annurev-med-041709-133809
10. Packard RRS, Libby P (2008) Inflammation in atherosclerosis: from vascular biology to biomarker discovery and risk prediction. Clin Chem 54:24–38. https://doi.org/10.1373/clinchem.2007.097360
11. Brown TM, Bittner V (2009) Biomarkers of atherosclerosis: clinical applications. Curr Cardiovasc Risk Rep 3:23–30. https://doi.org/10.1007/s12170-009-0005-z
12. Alexopoulos N, Raggi P (2009) Calcification in atherosclerosis. Nat Rev Cardiol 6:681–688. https://doi.org/10.1038/nrcardio.2009.165
13. Li X, Heber D, Gonzalez JC et al (2017) Association between osteogenesis and inflammation during the progression of calcified plaque evaluated by ^{18}F-fluoride and ^{18}F-FDG. J Nucl Med 58:968–974. https://doi.org/10.2967/jnumed.116.182790
14. Izquierdo-Garcia D, Davies JR, Graves MJ et al (2009) Comparison of methods for magnetic resonance-guided [18-F] fluorodeoxyglucose positron emission tomography in human carotid arteries: reproducibility, partial volume correction, and correlation between methods. Stroke. 40(1):86–93. https://doi.org/10.1161/STROKEAHA.108.521393
15. Agatston AS, Janowitz WR, Hildner FJ et al (1990) Quantification of coronary artery calcium using ultrafast computed tomography. J Am Coll Cardiol 15:827–832. https://doi.org/10.1016/0735-1097(90)90282-T
16. Ohya M, Otani H, Kimura K et al (2011) Vascular calcification estimated by aortic calcification area index is a significant predictive parameter of cardiovascular mortality in hemodialysis patients. Clin Exp Nephrol 15:877–883. https://doi.org/10.1007/s10157-011-0517-y
17. Van Der Bijl N, Joemai RMS, Geleijns J et al (2010) Assessment of Agatston coronary artery calcium score using contrast-enhanced CT coronary angiography. Am J Roentgenol 195:1299–1305. https://doi.org/10.2214/AJR.09.3734
18. Macnab JJ, Miller LT, Polatajko HJ (2001) The search for subtypes of DCD: is cluster analysis the answer? Hum Mov Sci 20(1–2):49–72. https://doi.org/10.1016/S0167-9457(01)00028-8
19. Rutland M, Que L, Hassan IM (2000) "FUR"—one size suits all. Eur J Nucl Med 27:1708–1713. https://doi.org/10.1007/s002590000337
20. Ishizu K, Nishizawa S, Yonekura Y et al (1994) Effects of hyperglycemia on FDG uptake in human brain and glioma. J Nucl Med 35:1104–1109
21. Rudd JH, Myers KS, Bansilal S et al (2007) (18)Fluorodeoxyglucose positron emission tomography imaging of atherosclerotic plaque inflammation is highly reproducible: implications for atherosclerosis therapy trials. J Am Coll Cardiol 50:892–896. https://doi.org/10.1016/j.jacc.2007.05.024
22. Kitagawa T, Yamamoto H, Toshimitsu S et al (2017) 18F-sodium fluoride positron emission tomography for molecular imaging of coronary atherosclerosis based on computed tomography analysis. Atherosclerosis 263:385–392. https://doi.org/10.1016/j.atherosclerosis.2017.04.024
23. Bentourkia M (2003) PET kinetic modeling of 11C-acetate from projections. Comput Med Imaging Graph 27:373–379. https://doi.org/10.1016/S0895-6111(03)00018-1
24. van den Hoff J, Oehme L, Schramm G et al (2013) The PET-derived tumor-to-blood standard uptake ratio (SUR) is superior to tumor SUV as a surrogate parameter of the metabolic rate of FDG. EJNMMI Res 3(1):77. https://doi.org/10.1186/2191-219X-3-77
25. Thie JA (2004) Understanding the standardized uptake value, its methods, and implications for usage. J Nucl Med 45:1431–1434
26. Torizuka T, Nobezawa S, Momiki S et al (2000) Short dynamic FDG-PET imaging protocol for patients with lung cancer. Eur J Nucl Med 27(10):1538–1542. https://doi.org/10.1007/s002590000312
27. Bentourkia M (2003) PET kinetic modeling of^{11}C-acetate from projections. Comput Med Imaging Graph 27(5):373–379. https://doi.org/10.1016/S0895-6111(03)00018-1
28. Christensen AN, Reichkendler MH, Larsen R et al (2014) Calibrated image-derived input functions for the determination of the metabolic uptake rate of glucose with [18F]-FDG PET. Nucl Med Commun 35:353–361. https://doi.org/10.1097/MNM.0000000000000063
29. Croteau E, Lavallée É, Labbe SM et al (2010) Image-derived input function in dynamic human PET/CT: methodology and validation with 11C-acetate and 18F-fluorothioheptadecanoic acid in muscle and 18F-fluorodeoxyglucose in brain. Eur J Nucl Med Mol Imaging 37:1539–1550. https://doi.org/10.1007/s00259-010-1443-z
30. Lodge MA, Chaudhry MA, Wahl RL (2012) Noise considerations for PET quantification using maximum and peak standardized uptake value. J Nucl Med. https://doi.org/10.2967/jnumed.111.101733

31. Tahara N, Kai H, Ishibashi M et al (2006) Simvastatin attenuates plaque inflammation: evaluation by fluorodeoxyglucose positron emission tomography. J Am Coll Cardiol 48:1825–1831. https://doi.org/10.1016/j.jacc.2006.03.069
32. Maldonado N, Kelly-Arnold A, Laudier D et al (2015) Imaging and analysis of microcalcifications and lipid/necrotic core calcification in fibrous cap atheroma. Int J Cardiovasc Imaging 31:1079–1087. https://doi.org/10.1007/s10554-015-0650-x
33. Wenk JF, Papadopoulos P, Zohdi TI (2010) Numerical modeling of stress in stenotic arteries with microcalcifications: a micromechanical approximation. J Biomech Eng 132:091011. https://doi.org/10.1115/1.4001351
34. Burke AP, Kolodgie FD, Farb A et al (2002) Morphological predictors of arterial remodeling in coronary atherosclerosis. Circulation 105:297–303
35. Wu Y-W, Kao H-L, Chen M-F et al (2007) Characterization of plaques using 18F-FDG PET/CT in patients with carotid atherosclerosis and correlation with matrix metalloproteinase-1. J Nucl Med 48:227–233
36. Kwee RM, Teule GJ, van Oostenbrugge RJ et al (2009) Multimodality imaging of carotid artery plaques: 18F-fluoro-2-deoxyglucose positron emission tomography, computed tomography, and magnetic resonance imaging. Stroke 40:3718–3724. https://doi.org/10.1161/strokeaha.109.564088